Original Article

Role of diffusion weighted MR imaging in characterization of focal kidney and upper urinary tract lesions

CrossMark

Donia M. Sobh (MBBch, MD) [a,*], Prof. Dr. Galal El Sayed Magdy El Hawary (MBBch, MD) [a],
Prof. Dr. Mohamed Abou El Ghar (MBBch, MD) [b], Prof. Dr. Tarek Abd El Moneim El-Diasty [b],
Prof. Dr. Magdy El-Sayed Settein [a], Dr. Shereen ElShaer [c],
Prof. Dr. Mohamed Salah Ebrahim Tantawy [a]

[a] Diagnostic Radiology, Faculty of Medicine, Mansoura University, Egypt
[b] Diagnostic Radiology Urology and Nephrology Center, Egypt
[c] Public Health and Community Medicine, Egypt

ARTICLE INFO

ABSTRACT

Previous studies suggested that the apparent diffusion coefficient (ADC) value could help in the differentiation and characterization of the benign and malignant renal masses. However, there is still wide overlap in the ADC values between the benign and malignant tumors.

Objectives: To retrospectively assess the usefulness of the diffusion weighted imaging (DWI) for the characterization and differentiation between benign and malignant renal masses.

Methods: A total of 87 renal and/or upper ureteric masses were included in our study. The signal intensity of the lesions was assessed on both the DWI and ADC map and the ADC value was calculated. *t* test, ANOVA test and Receiver operating characteristic (ROC) curve analysis were performed.

Results: The ADC values of benign lesions were significantly higher than those of the malignant masses [3.2 versus 1.3×10^{-3} mm^2/s], Median, P < 0.0001. The sensitivity and specificity of the DWI for the differentiation of benign and malignant masses were 98% and 73% using an ADC cutoffvalue of 2.2. Clear cell renal cell carcinoma demonstrates higher ADC value than non clear cell RCC.

Conclusion: DWI-MRI has a role in differentiation of benign and malignant renal masses and the characterization of different malignant categories, subtypes and grades.

© 2016 The Egyptian Society of Radiology and Nuclear Medicine. Production and hosting by Elsevier. This is an open access article under the CC BY-NC-ND license (http://creativecommons.org/licenses/by-nc-nd/4.0/).

1. Introduction

Noninvasive methods including CT and MRI play a vital role in the diagnosis and characterization of renal masses.

The choice of treatment varies between reassurance of the patient, radiological follow-up, ablative procedures, and partial and radical nephrectomy [1].

The conventional CT and MRI sequences cannot easily differentiate benign from malignant lesions in many cases. Studies have shown that 16–33% of nephrectomies are performed on benign lesions [1].

There is also a strong need for alternatives to gadolinium-enhanced sequences in patients at risk for nephrogenic systemic fibrosis (NSF) [2].

Diffusion weighted imaging (DWI) is based on the detection of the Brownian motion of free water molecules in tissue, which has been shown to be inversely proportional to cellular density [3].

DWI is widely used in brain imaging and has been proved to be of great value [3]. The recent advancement in MRI equipment allowed the application of the DWI in abdominal imaging [3].

DWI provides qualitative and quantitative information on tissue characterization without the need for gadolinium administration [4].

Previous studies on the renal neoplasms suggested that the apparent diffusion coefficient (ADC) value could help in the differentiation and characterization of the benign and malignant renal masses [4].

However to our knowledge, there is still wide overlap in the ADC values between the benign and malignant renal tumors [5].

There is no enough data on whether the apparent diffusion coefficient (ADC) value of the diffusion weighted imaging (DWI) can help in the characterization of the RCC pathological subtypes and grades [6].

The aim of this study was to retrospectively assess the usefulness of the diffusion weighted imaging (DWI) for the differentiation between benign and malignant renal masses, characterization of the different subtypes and grades of RCC, as well as the characterization of the different grades of TCC.

2. Patients & methods

This retrospective research was approved by our institutional medical review board. Patients' consent was waived.

2.1. Inclusion and exclusion criteria

163 consecutive patients (with 173 renal and/or upper ureteric lesions) were initially included in our study. Most of these patients underwent MRI, follow-up, and definitive management, including biopsy or surgical excision for renal neoplasms. We retrospectively reviewed the MRI examinations and pathological results for these patients.

For our patients, MRI was performed prior to the biopsy and before any tumor therapy was given.

We included only the cases that have final diagnosis available on our database. As regards the presumed simple or mildly complex cystic lesion (Bosniak I and II categories), we included the cases that have at least 2-years follow-up imaging as confirmation of stability.

We excluded the lesions that were missing the definitive imaging/clinical diagnosis or histopathological confirmation (n = 50), the lesions that did not have the diffusion weighted MRI sequence (n = 32), and the lesions in which the diffusion weighted MRI was not interpretable due to poor quality and obvious artifact (n = 4).

Finally, total of 79 patients with 87 lesions were included in our study.

2.2. MRI protocol

MRI was performed using a 1.5 T MRI unit (Signa horizon LX echo speed, General Electric Medical Systems, Milwaukee, USA) using phased array surface body coil.

The following sequences were provided with respiratory triggering: Axial spin echo (SE) T1-weighted imaging, axial and coronal fast spin echo (FSE) T2 weighted imaging, and axial or coronal in and out of phase.

The Diffusion weighted imaging (DWI) sequence was done in both the coronal and axial planes. This sequence was obtained by single-shot spin echo planar imaging (SE-EPI) using the following parameters: TR/TE: 8000/74–104 ms, slice thickness, 5 mm, interslice gap, 0 mm, FOV, 42–46 and matrix: 128/128. B factor of 0 and 800 s/mm^2 was used to calculate the ADC value.

Using the spoiled gradient echo (SGE) sequence in the axial and coronal planes, **multiphase dynamic post contrast-enhanced (DCE) MR images** were obtained. Contrast enhanced MRI was not performed in 11 of our patients; because of reduced GFR in 10 and pregnancy in one patient.

2.3. Image analysis

2.3.1. DWI and ADC tumor signal (qualitative assessment)

The signal intensity of each lesion was scored both in the ADC and DWI images using a 3-point rating scale compared with contralateral parenchyma where 1 = hyperintense, 2 = hypointense and 3 = isointense or mixed signal.

2.3.2. Quantitative assessment of the ADC map

The DWI images were transferred to an independent workstation (General electric) for postprocessing, and the ADC maps were reconstructed.

The mean ADCs (±standard deviations) of each lesion were measured from the ADC maps with average sized circular ROIs placed as follows:

For homogenous solid tumors, we chose the largest possible ROI.

For heterogenous solid lesions, more than one ROI were placed and the average ADC value was calculated.

As regards the solid tumors containing cystic necrosis, 2 ROIs were placed: one in the solid part and a second ROI in the cystic component. For the complex cystic lesions, the ROI was placed in the solid nodule or in the thick septations.

The ADC images were reviewed in correlation with the T1, T2 and post contrast images if available. This helped optimum ROI placement.

2.3.3. Lymphadenopathy

In positive cases, the DWI and ADC images were reviewed to assess the signal intensity and ADC values for the enlarged LNs.

2.4. Reference standard

The definitive diagnosis was made by histopathological examination. For lesions demonstrating typical benign radiological features, the benign nature was confirmed by at least 2-year interval stability.

2.5. Statistical analysis

The data were collected, coded, processed and analyzed using SPSS ver 16 (statistical package for social sciences). Descriptive statistics (mean (M), standard deviation (SD), frequencies and percentages) were calculated.

When the data were parametric the Student's t-test was used in comparison with two groups while ANOVA test was used in the case of more than two groups examined. Relationships between categorical and continuous variables were examined using the Mann–Whitney U-test for two ordered categorical variables.

Receiver operating characteristic (ROC) curve analysis was used to compare diagnostic capabilities.

3. Results

A total of 87 lesions in 79 patients with renal and/or upper ureteric masses were finally enrolled in our study (69 male patients with 76 lesions and 10 female patients with 11 lesions). The age range in our cases was 3–84 years. The median age was 63 years.

The final diagnosis was proved by pathological examination (biopsy or nephrectomy) in 73 lesions. Lesions demonstrated typical radiological benign features such as AML (n = 1), simple cyst (n = 10), and mildly complex cysts (n = 3). The benign nature was confirmed by at least 2 years of interval stability.

3.1. Study groups

These lesions were subdivided into 3 categories based on their location and nature as follows:

3.1.1. Group 1: Cystic renal parenchymal masses

This group includes 22 lesions (18 benign and 4 malignant). These lesions were categorized according to the Bosniak classification as follows: Bosniak grade I (n = 10), Bosniak II (n = 3), Bosniak IIF (n = 2), Bosniak III (n = 5) and Bosniak IV (n = 2).

3.1.2. Group 2: Solid renal parenchymal masses

This group includes 34 lesions (5 benign and 29 malignant).

3.1.3. Group 3: Urothelial lesions

This group includes a total of 31 TCC lesions (calyceal (n = 23), renal pelvis (n = 2) and upper ureteric (n = 6) (Fig. 1 for all lesions in our study).

3.2. Diffusion weighted MRI

All the 87 lesions were clearly identified on the DWI images. The quality of DW images was good in all patients (Table 1 for the signal intensity of the different lesions on the DWI and ADC.

Four of the malignant lesions had metastatic renal hilar and/or paraaortic LNS that were clearly identified on the DWI as bright lesions.

16 out of the 22 *cystic lesions* demonstrated low signal intensity on the DWI images at b 800. Three out of the four malignant cystic lesions demonstrated low signal intensity on both the DWI and ADC images.

Among the 29 **malignant solid parenchymal renal lesions**, 20 lesions demonstrated high signal intensity on the DWI with corresponding low signal intensity on the ADC map in keeping with reduced diffusion.

7 lesions demonstrated mixed signal intensity on both the DWI and the ADC images, which is attributed to the mixed components. 3 of these lesions with the mixed signal were **clear cell renal cell carcinoma (CCRCC),** 2 lesions were unclassified RCC and one lesion was lymphoma.

All the *urothelial lesions* in our study (n = 31) were histologically malignant and transitional cell carcinoma type.
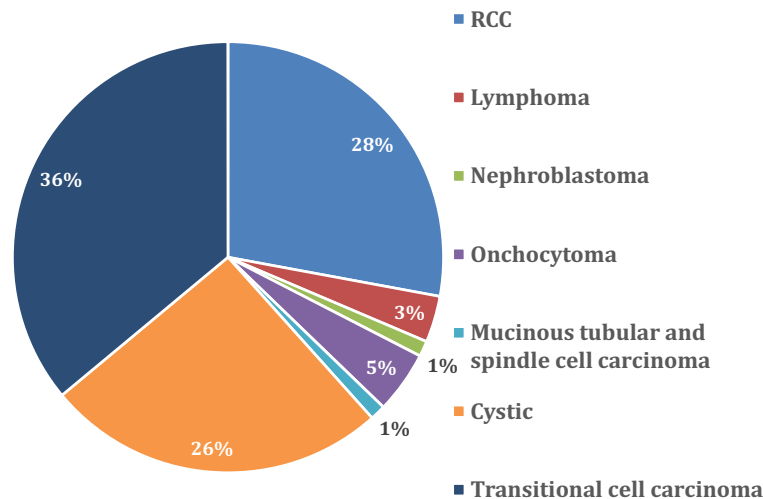

- RCC
- Lymphoma
- Nephroblastoma
- Onchocytoma
- Mucinous tubular and spindle cell carcinoma
- Cystic
- Transitional cell carcinoma

Fig. 1. Pie representation of all lesions included in our study.

Table 1
The signal intensity of the different lesions on the DWI (b800) and ADC images.

	No	Solid	Cystic	Urothelial
Signal intensity on the DWI				
Bright	58	24	3	31
Low	19	3	16	0
Mixed	10	7	3	0
Signal intensity on the ADC				
Bright	17	3	14	0
Low	60	24	5	31
Mixed	10	7	3	0

Table 2
ADC values of all renal lesions.

Lesion	No	ADC $\times 10^{-3}$ mm^2/s (mean ± SD)
Cystic	22	2.4 ± 1.4
Solid renal parenchymal		
AML	1	0.6
Nephroblastoma	1	1.9
Oncocytoma	4	2.4 ± 0.4
RCC	24	1.3 ± 0.6
Lymphoma	3	1.2 ± 0.4
Mucinous tubular and spindle cell carcinoma	1	0.9
Urothelial: transitional cell carcinoma	31	1.4 ± 0.3

These lesions demonstrated bright signal on the DWI and low signal intensity on the ADC image.

3.2.1. Benign versus malignant

Among the 87 lesions in this study, the total number of benign lesion was 23, while the total number of malignant lesion was 64 (Table 2 for ADC values of all lesions in this study).

The ADC values of benign lesions were significantly higher than those of malignant masses [3.2 (0.3–3.7) versus 1.3 (0.3–2.9) $\times 10^{-3}$ mm^2/s), Median (Min–Max) respectively, P < 0.0001] (Fig. 2).

In our study, ROC analysis was done twice to differentiate malignant from benign renal lesions. AML was excluded from both ROC curves to improve the specificity.

The first ROC curve included all the solid and cystic parenchymal and urothelial lesions. The sensitivity and specificity were 98% and 73% respectively using ADC cutoff value of 2.2 for the differentiation between malignant and benign renal lesions (Fig. 3).

The second ROC curve included only the solid renal parenchymal and urothelial lesions. The sensitivity and specificity were 98% and 75% respectively using ADC cutoff value of 2.18 (Fig. 4).

3.3. Cystic renal masses

The ADC values for the benign cystic lesions were significantly higher compared with the malignant cystic lesions 3.35 (0.32–3.7) $\times 10^{-3}$ versus 0.63 (0.46–0.92) $\times 10^{-3}$ mm^2/s [Median (Min–Max)] respectively (Tables 3 and 4).

The lesions of higher Bosniak categories demonstrated lower ADC value and most of them were malignant in nature. In our study, the ADC values for Bosniak categories I, II, IIF, III were 3.49 ± 0.16, 2.43 ± 1.15, 1.65 ± 0.49 and 0.50 ± 0.25 $\times 10^{-3}$ mm^2/s respectively. However, in our study, grade IV had a mean ADC value of 2.09 ± 1.85, and the accuracy of this value is questionable due to the limited number of cases in this category.

3.3.1. Benign cystic lesions and cystic necrosis in malignant renal masses

Among the solid malignant masses in our study, 7 lesions demonstrated cystic necrosis. We measured the ADC value of that cystic part separate from the solid component.

The ADC values for the cystic component were significantly lower compared with the benign cystic lesions of 2.2 versus 3.35 $\times 10^{-3}$ mm^2/s respectively (Table 5).

3.4. Solid renal parenchymal masses

The ADC values for the solid malignant renal parenchymal masses were significantly lower compared with the benign solid parenchymal masses after exclusion of the AML.

3.4.1. Characterization of the RCC subtypes

The ADC values for the clear cell RCC (CCRCC) were significantly higher than those of the papillary RCC [1.8 (0.8–2.9) versus 0.9 (0.3–1.9), median (min–max)] respectively, p = 0.008. There was no significant difference between the remaining RCC subtypes (Table 6).

Due to small number of lesions in each of the RCC subtype, we combined the papillary, chromophobe and unclassified RCC in one group as non clear cell RCC (non-CCRCC) and re-compared it to the ADC values for the CCRCC (Table 7).

The ADC value for the CCRCC was 1.8 $\times 10^{-3}$ versus 1.04 $\times 10^{-3}$ mm^2/s [Median (Min–Max)] for the non-CCRCC.

3.4.2. Characterization of the RCC grade

We calculated the ADC values for the different RCC grades. Both solid RCC and cystic RCC were included in this comparison.

The ADC values for grades I, II and III were 1.3 (0.3–1.66), 1.2 (0.8–2.97) and 0.9 (0.31–1.38) $\times 10^{-3}$ mm^2/s respectively (Table 8).
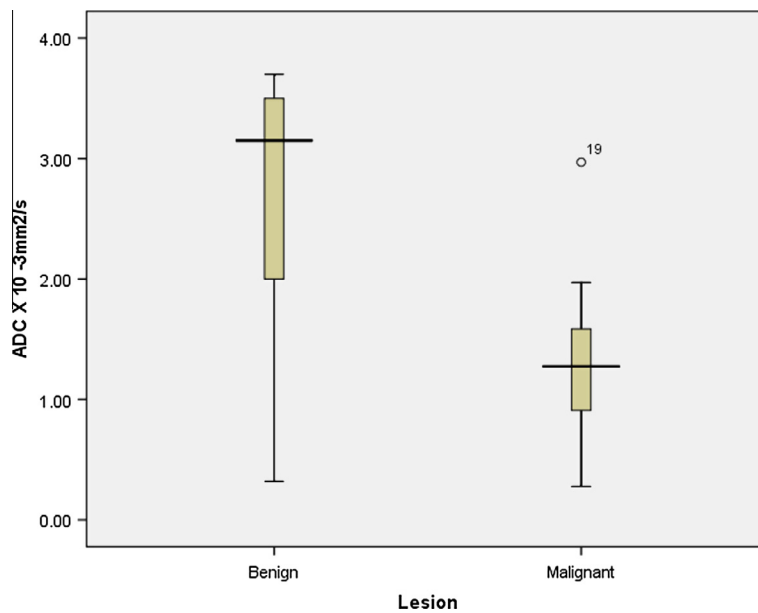
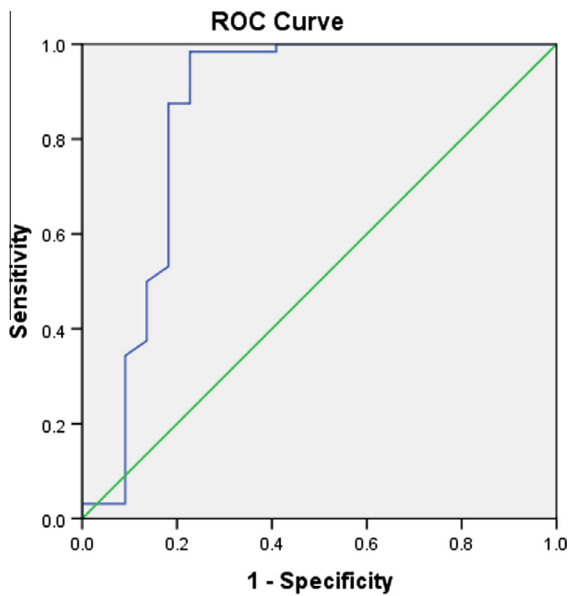**Fig. 2.** Box-and-whisker plots of benign and malignant renal lesions (excluding AML).

Fig. 3. ROC curve shows the performance of DWI for differentiating benign from malignant solid and cystic renal neoplasm.
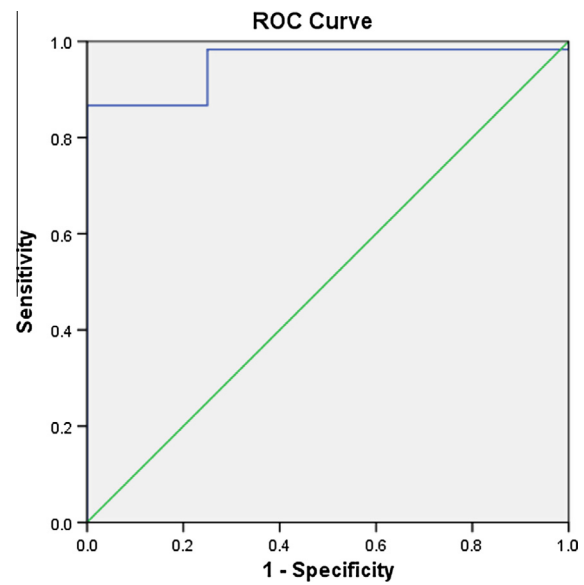

Fig. 4. ROC curves show performance of DWI for differentiating benign from malignant solid parenchymal and upper urothelial renal lesions.

3.4.2.1. Urothelial lesions. All the urothelial lesions in our study were malignant of the transitional cell carcinoma type. The mean ADC value for the TCC was $1.4 \pm 0.3 \times 10^{-3}$ mm^2/s.

4. Discussion

In our study, most of the **solid malignant lesions** demonstrated bright signal on the DWI image with corre-

Table 3
The mean ADC values of the different categories of cystic renal masses.

Lesion type	No	Bosniak category	ADC $\times 10^{-3}$ mm^2/s
Simple cyst	10	I	3.49 ± 0.16
Mildly complicated cyst	3	II	2.73 ± 0.64
Chronic abscess	3	III	0.33 ± 0.01
Hemorrhagic cyst	2	IIF	2.35 ± 1.48
Cystic renal carcinoma	4	III & IV	0.66 ± 0.23

Table 4
The ADC values of benign and malignant cystic lesions.

Cystic, parenchymal	No	ADC $\times 10^{-3}$ mm^2/s median (Min–Max)	Test of significance
Benign	18	3.35 (0.32–3.7)	Z = 2.4
Malignant	4	0.63(0.46–0.92)	P = 0.01

Table 5
Benign cystic lesions versus malignant cystic necrosis.

Lesion	No	ADC $\times 10^{-3}$ mm^2/s Median (Min–Max)	Test of significance
Benign cystic lesions	18	3.35 (0.32–3.7)	Z = 2.06
Cystic necrosis	7	2.2 (0.5–3)	P = 0.03*

P = 0.03*: statistically significant.

Table 6
The mean ADC values for the different RCC subtypes.

Lesion	n = 24	
	No	ADC $\times 10^{-3}$ mm^2/s Mean ± SD
RCC type		
Clear cell	7	1.7 ± 0.7
Papillary	11	0.96 ± 0.5
Chromophobe	2	1.4 ± 0.4
Unclassified	4	1.2 ± 0.4

Table 7
The ADC values for the CCRCC and Non CCRCC.

Lesion	n = 24 ADC $\times 10^{-3}$ mm^2/s median (Min–Max)	Test of significance
RCC type		
Non clear cell	1.04 (0.3–1.9)	Z = 2.6
Clear cell	1.8 (0.8–2.9)	P = 0.008*

P = 0.008*: statistically significant.

Table 8
The ADC values of the different RCC grades.

Lesion	No	ADC $\times 10^{-3}$ mm^2/s
RCC grade		
I	5	1.3 (0.3–1.66)
II	15	1.2 (0.8–2.97)
III	8	0.9 (0.31–1.38)

sponding low signal on the ADC image. The bright DWI signal helped the identification of the lesion and determination of its extent.

Whereas, the majority of the **benign masses** demonstrated low signal on the diffusion weighted images, **most of the benign lesions in this study were of cystic nature.** Some of the benign lesions demonstrated high signal on the DWI but in most of these cases this was attributed to the T2 shine through effect and these lesions showed high signal on the ADC map as well.

The ADC is a quantitative parameter that detects the extent of diffusion of water molecules. It is computed from DW-MRI [7].

Multiple **b values** are used in the clinical practice to increase the accuracy of the ADC calculation. Many studies suggested that using b value higher than 400 s/mm^2 for abdominal diffusion MRI scans gives more accurate ADC measurement as it reduces the T2 shine through and intra-voxel perfusion effect [8,9].

On the other hand, higher b values reduce the signal to noise ratio and result in anatomic distortion [8,10,11].

Wu et al. found that a b-value of 1500 s/mm^2 significantly improved the specificity, but not the sensitivity, in diagnosing upper urinary tract cancer compared to a b-value of 500 s/mm^2 S [11].

Bozcurt et al. found that a b-value of 800 s/mm^2 increased specificity with no significant effect on sensitivity and accuracy compared to a b-value of 400 s/mm^2 [12].

We used a b value of 800 s/mm^2 as part of our standard renal mass MRI protocol.

In general, we found that the ADC values for the **cystic lesions** are higher than those of the solid lesions.

Simple cysts have the highest ADC value, because of their high water content which allows unrestricted diffusion [13]. The mean ADC value for simple renal cysts in our study was 3.49 ± 0.16, which is close to a study by Zhang et al. (3.269 ± 0.61 $\times 10^{-3}$ mm^2/s) [14].

This is slightly higher than the result of Inci et al., who reported mean ADC value of 3.09 ± 0.14 $\times 10^{-3}$ mm^2/s in Bosniak I category [15].

Similar to previous studies, the ADC values for the benign cystic lesions in our study are significantly higher compared with the malignant cystic lesions (Table 4).

In our study, the ADC values for the mildly complicated (Bosniak II) and the hemorrhagic cysts are 2.73 ± 0.64 $\times 10^{-3}$ mm^2/s and 2.35 ± 1.48 $\times 10^{-3}$ mm^2/s respectively. These results are in agreement with a study by Zhang et al., which showed an ADC value of 2.6 ± 0.4 $\times 10^{-3}$ mm^2/s for the hemorrhagic renal cysts [14].

Similar to previous studies, we found that the ADC value of renal abscess is low 0.33 ± 0.01 $\times 10^{-3}$ (Fig. 5).

We found that as the complexity of the renal cysts increases (higher Bosniak categories), the ADC values decrease as these lesions are more likely to be malignant (Table 3).

In our study, grade IV had a mean ADC value of 2.09 ± 1.85, the accuracy of this value is questionable due to the limited number of cases in this category.

In a study by Göya et al., the mean ADC value of Bosniak Category I cysts was 2.93 ± 0.14 $\times 10^{-3}$ mm^2/s in, which is relatively lower than that in our study [13].

The mean ADC value for Bosniak Category II cysts in that study by Goya et al., was 2.49 ± 0.30 $\times 10^{-23}$ mm^2/s, and they found that the mean ADC value of Bosniak Category III cysts was 1.95 ± 0.27 $\times 10^{-3}$ mm^2/s [13].

We found that there is a significant difference between grade I and grade II Bosniak categories (P = 0.01), between grade I and III (P = 0.002) and also between grade II and III (P = 0.02). These results are concordant with the study of Goya et al. [13].
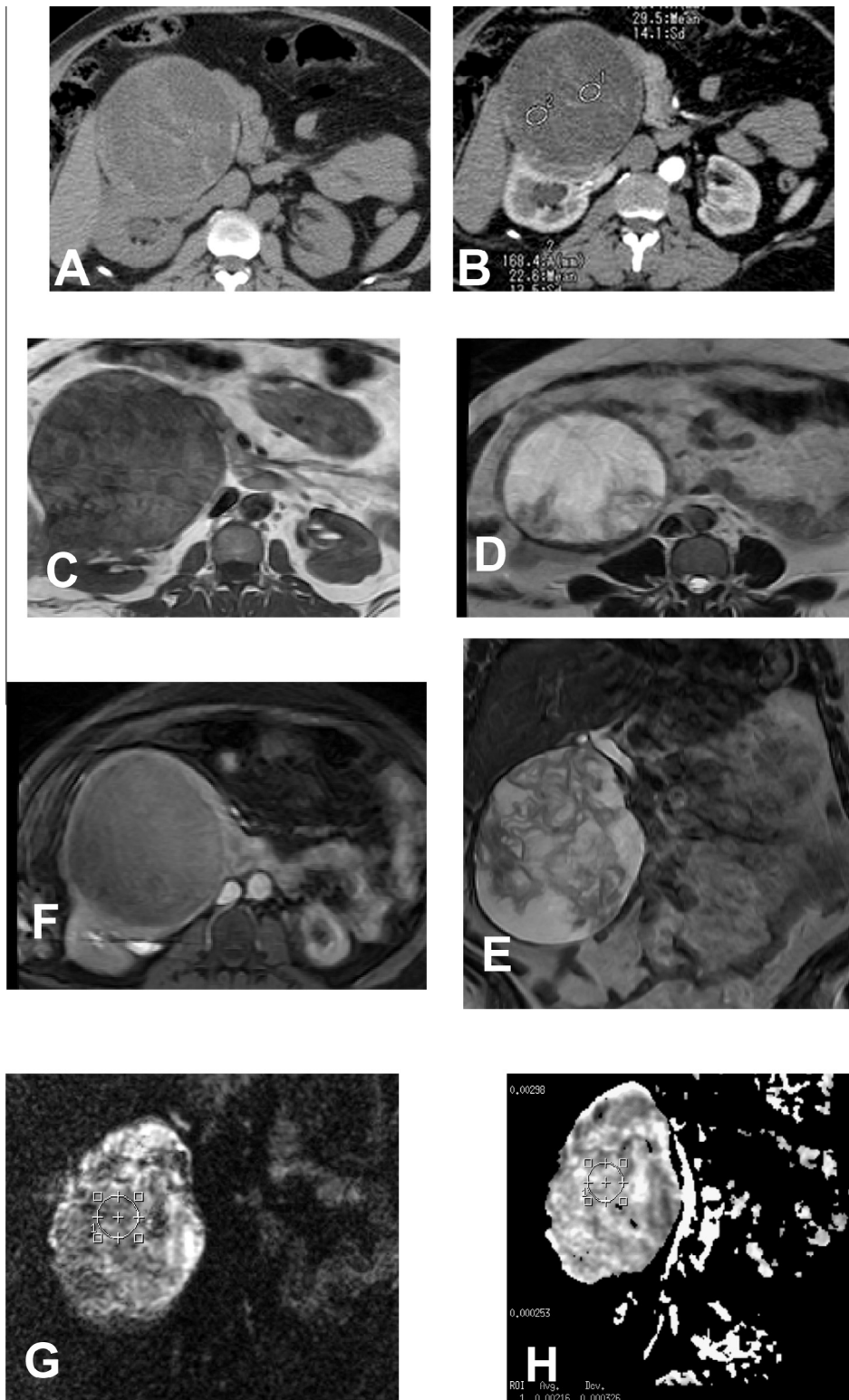
Fig. 5. Chronic abscess (confirmed surgically). (A and B) Non and post contrast axial CT images demonstrating a large peripherally enhancing complex mass arising from and posteriorly displacing the right kidney. Hyperdense content is identified within the mass. (C) Axial T1 FSE. (D and E) Axial and coronal T2 FSE: The mass displays heterogenous signal on both T1 and T2 images with internal debris. (F) Axial post contrast SGRE: The mass demonstrates thick rim peripheral enhancement. (G and H) DWI and ADC map in the coronal plane reveal reduced diffusion within the mass, and the ADC value is 0.32×10^{-3} mm^2/s.
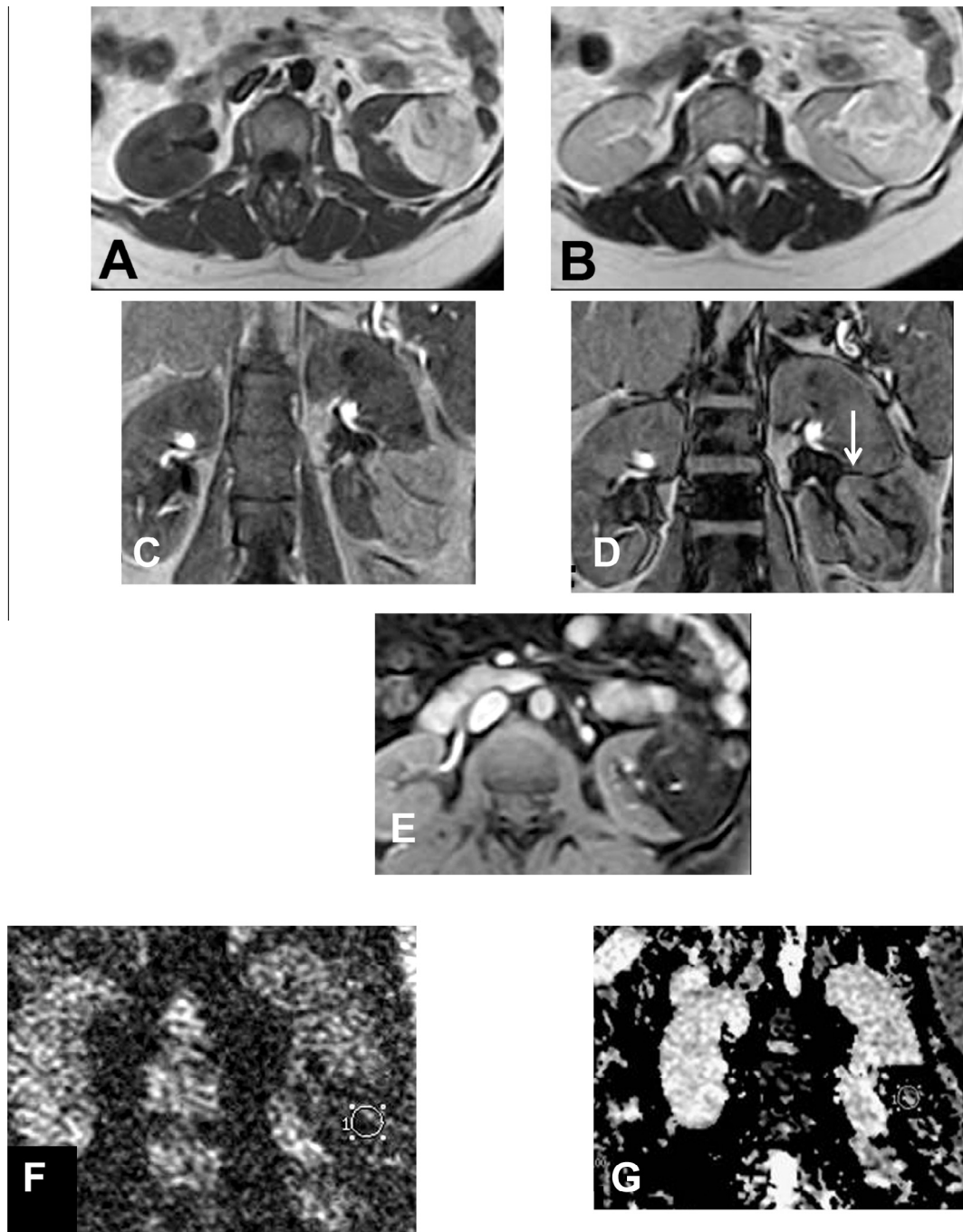
Fig. 6. 51-year old female patient with a left renal mass. (A) Axial spin echo T1WI: The mass is hyperintense with signal intensity similar to the subcutaneous and retroperitoneal fat. (B) Axial T2 FSE: The mass is predominantly hyperintense with few hypointense streaks. (C and D) Coronal in and out of phase images: The mass is hyperintense on the in phase image (C) with no significant drop of its signal on the out of phase (D) image. Note the chemical shift artifact at fat water interface (arrow in D). (E) Axial T1 Post contrast SPGR shows complete loss of the high signal of the mass which confirms the presence of macroscopic fat. (F) DWI (b = 800 s/mm^2): The mass is hypointense to the adjacent renal parenchyma, (G) ADC map: the ADC value of the lesion was 0.56×10^{-3} mm^2/s. The definitive imaging diagnosis was angiomyolipoma.

We did not find any significant statistical difference between IIF and I, IIF and II, IIF and III or III and IV Bosniak categories. The accuracy of these results needs to be assessed by future studies including larger number of cases.

4.1. Cystic necrosis versus benign cysts

Zhang et al., found that the cystic necrosis, unlike benign cyst, shows reduced diffusion and lower ADC values even though they can both display similar appearance on
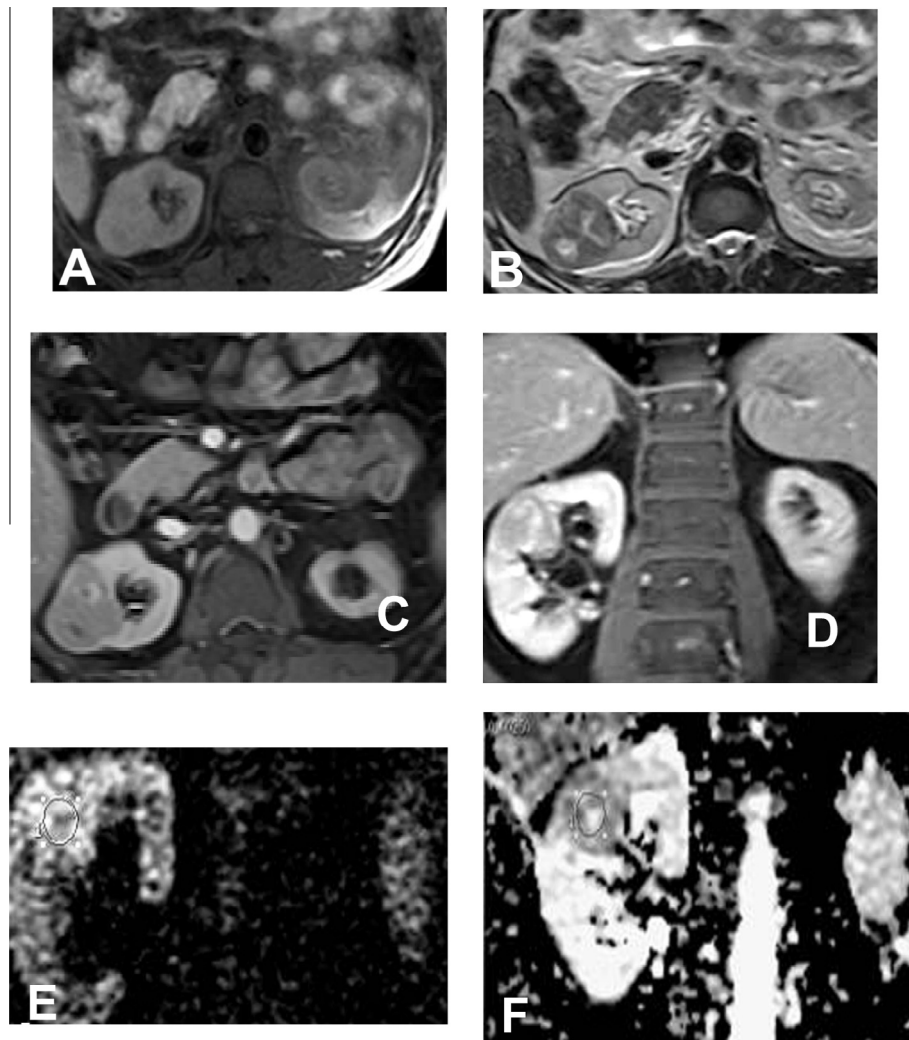
Fig. 7. Oncocytoma. (A) Axial T1WI. (B) Axial T2 WI. (C and D) Axial and coronal post contrast T1. The mass displays heterogenous signal with mild enhancement and areas of central necrosis. (E and F) DWI and ADC map on the coronal plane: The mass demonstrates reduced diffusion with bright signal on the DWI and low signal on the ADC map. The ADC value is 2×10^{-3} mm^2/s.

conventional MR images. This is explained by the solid nature of the cystic necrosis, which is made of non-enhancing nonviable tissue [14].

Our results are in agreement with the prior studies. The ADC values for the malignant cystic component were significantly lower compared with the benign cystic lesions (Table 5).

Sevcenco et al., found no significant differences between the ADC values of **benign and malignant solid renal lesions** using 3T MRI. Benign cystic lesions were excluded from Sevcenco et al.'s study [16].

However, a meta-analysis by Liu et al., found that the ADC values of malignant renal lesions were markedly lower than those of benign renal lesions [4].

Our results are in agreement with this meta-analysis. In our study, the ADC values of the malignant lesions (solid and cystic) were significantly lower than those of the benign renal masses [1.3 (0.3–2.9) versus 3.2 (0.3–3.7) ×

10^{-3} mm^2/s], Median (Min–Max) respectively, P < 0.0001 (Fig. 2).

A study by Doagany et al., which included both solid and cystic renal parenchymal lesions (excluding AML) showed cutoff values of 2.36 for b value of 600, and 2.27 for b value of 1000 to differentiate malignant from benign renal lesions. For b values of 600, and 1000 s/mm^2, the sensitivity was 71% and 90%, and the specificity was 91% and 73% respectively [8].

Angiomyolipoma (AML) is a benign renal neoplasm that is composed of variable amounts of fat, abnormal blood vessels and muscles.

As demonstrated in many previous studies, the ADC value of AML is low, particularly the fat rich ones, mimicking malignant lesions. The ADC value of our AML case was 0.6×10^{-3} mm^2/s, which is even significantly lower than RCC. These results are similar to those of the previous studies including a study by Yoshikawa et al. [9].
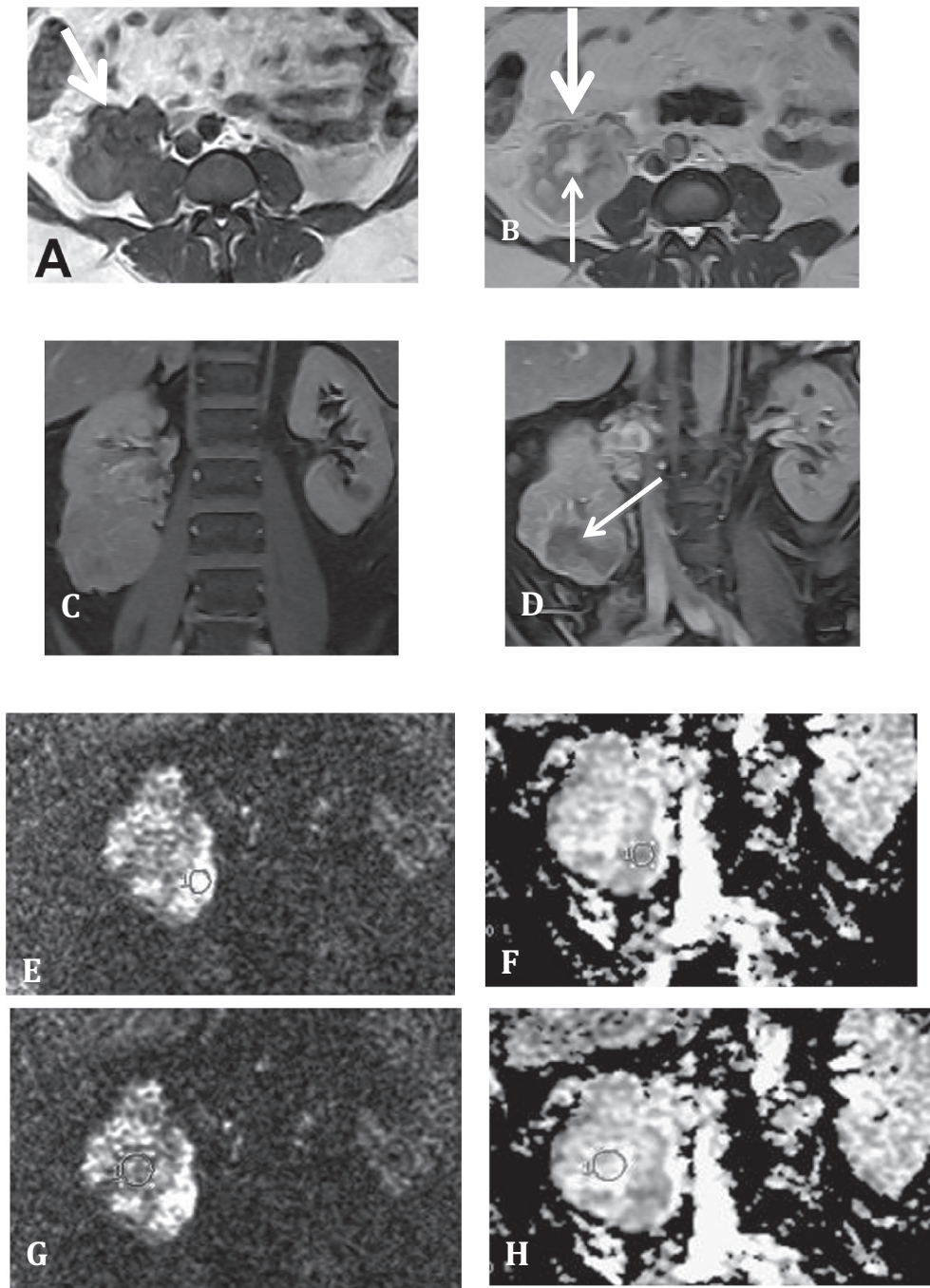
Fig. 8. RCC (clear cell subtype). 59-year old male patient with a complex solid mass in the lower pole of the right kidney. (A and B) Axial T1 and T2 FSE at the level of the exophytic mass (thick white arrow an (a & b)). Note the T2 hyperintense central necrosis (thin white arrow in b). (C and D) Coronal post contrast SGRE: The solid part of the mass enhances heterogeneously with non enhancing central necrosis (thin white arrow in d). (E and F) DWI and ADC map in the coronal plane: The ROI was placed in the solid part which demonstrates restricted diffusion and ADC value of 1.38×10^{-3} mm^2/s. (G and H) A second ROI was placed in the cystic necrosis which has ADC value of 2.1×10^{-3} mm^2/s (higher than the solid part but lower than simple cysts).

The low ADC value of AML is attributed to its abundant fat content. Inci et al., observed decreasing ADC values of angiomyolipomas with inverse correlation of the fatty content [15].

Accurate diagnosis of AML can be made by reviewing the conventional MR images. We should be aware that the DW MR is misleading in this benign category (Fig. 6).

We had 4 cases of **oncocytoma** in our study. The mean ADC value for these lesions was 2.4 ± 0.4 mm^2/s (Fig. 7). This is slightly higher compared to a study by Zhang et al., where the mean ADC value for oncocytoma was $2.16 \pm 0.02 \times 10^{-3}$ mm^2/s [14].

In our study, ***renal cell carcinoma (RCC)*** had a low ADC value $1.3 \pm 0.6 \times 10^{-3}$ mm^2/s. This is similar to previous studies. For example, in a study by Yu et al., the ADC value of RCC was $1.381 \pm 0.4 \times 10^{-3}$ mm^2/s [17].

RCC is classified into several ***subtypes*** based on the histopathological appearance, clinical course and the presence of abnormal genetic patterns. These subtypes include CCRCC, papillary, chromophobe and unclassified RCC [4] (see Fig. 8).

CCRCC has a worse prognosis than chromophobe or papillary RCC. It is important to differentiate the various subtypes of RCC as these subtypes respond differently to molecularly targeted therapies [17].

A study by Wang et al., showed that the sensitivity and specificity were 95.9% and 94.4% respectively to differentiate CCRCC from non-CCRCC by using DWI [18].

Yu et al. [17] concluded that there is a significant difference in the ADC value between the CCRCC and non-CCRCC (P = 0.001), CCRCC and chromophobe RCC (P < 0.001), and between CCRCC and papillary RCC (P = 0.002), respectively.

In our study, there was a significant difference between the ADC values of the CCRCC and papillary RCC (Table 6).

As suggested in many studies, the low ADC values of papillary RCC can be explained by the high cellularity which restricts the Brownian motion of water molecules within the tumor cells [16].

Unlike the previous studies, we found that there is no significant statistical difference between the CCRCC and the chromophobe or the unclassified RCC. This could be attributed to the small sample size in the non-CCRCC group in our study.

Similar to the previous studies, we found that there is a significant difference between the 2 groups with the CCRCC demonstrating higher ADC value compared with the non-CCRCC.

Studies by Rosenkrantz et al., and another study by Yu, et al. concluded that the ADC value of low grade RCC (grades I and II) is significantly higher than that of high-grade RCC (grades III and IV) [5,6].

We found that the ADC values were lower in most of our cases with high-grade RCC compared with low-grade lesions (Table 8).

The ADC value for grade III was the lowest. There was a statistical significant difference between grades II and III (P value = 0.04) but not between grades II and I. We did not have any grade IV lesions in our study.

All ***urothelial tumors*** in our groups (n = 31) were of the transitional cell carcinomas (TCC) type, which is the most common renal pelvis cancer.

We found that the mean ADC value of TCC is $1.4 \pm 0.3 \times 10^{-3}$ mm^2/s. This is slightly lower than the results of Paudyal et al., who reported an ADC value of $1.61 \pm 0.80 \times 10^{-3}$ mm^2/s for TCC [19].

A study by Paudyal et al., concluded that the ADC value for the RCC was significantly higher compared with the TCC. TCC is histologically composed of solid and densely

Table 9
Comparison between the ADC values of the different grades of TCC.

Lesion	No	ADC $\times 10^{-3}$ mm^2/s	Test of significance
TCC grade			
I$^\infty$	6	1.59 ± 0.19	One way ANOVA
II	15	1.36 ± 0.26	F = 3.4
III∞	10	1.22 ± 0.32	P = 0.05

$^\infty$ Significant difference (P = 0.03).

packed tumor cells with hypercellularity compared with RCC. In addition, RCC is frequently associated with the hemorrhage, necrosis and cystic parts. These may explain the higher ADC value of the RCC [19].

We found that the ADC values for the RCC were higher than TCC but the difference was not statistically significant.

To the best of our knowledge, there is no clear data about the value of DWI in differentiating the ***different grades of TCC***.

We found that the higher-grade TCC demonstrates lower ADC values.

There was statistical difference between grades I and III. Although The ADC values of most of the grade I lesions were lower than those of grade II, the difference was not statistically significant (Table 9).

Renal hilar and paraaortic LNs were identified in 5 of the malignant lesions in our study. These nodes were clearly identified by DWI as bright lesions and demonstrated low ADC values. Due to the small sample size, no statistical analysis could be performed for this group.

4.2. Study limitations

Our study has several potential limitations: first, the overall small size of the studied lesions particularly the small number of benign renal masses and second, the small number of each of RCC histological subtypes and grades.

Despite the small sample size, we were able to demonstrate significant difference between benign and malignant lesions.

Third, we did not study the combined use of DWI, contrast enhanced MRI, and MRI perfusion for the characterization of the renal masses, which probably will show higher sensitivities and specificities. Future studies can help further assessment of this combination.

5. Conclusion

Our study has shown that the DWI-MRI and the quantitative ADC measurements have a role in the differentiation of benign and malignant renal masses and the characterization of different malignant categories, subtypes and grades.

However, due to the overlap of the ADC values between certain renal lesions, the DWI should be used in correlation with the conventional MRI sequences.

Conflict of interest

We have no conflict of interest to declare.

References

[1] Sun MRM, Ngo L, Genega EM, Atkins MB, Finn ME, Rofsky NM, et al. Renal cell carcinoma: dynamic contrast-enhanced mr imaging for differentiation of tumor subtypes—correlation with pathologic findings 1. Radiology 2009;250(3):793–802.

[2] Taouli B, Thakur RK, Mannelli L, Babb JS, Kim S, Hecht EM, et al. Renal lesions: characterization with diffusion-weighted imaging versus contrast-enhanced MR imaging 1. Radiology 2009;251(2):398–407.

[3] Malayeri AA, El Khouli RH, Zaheer A, Jacobs MA, Corona-Villalobos CP, Kamel IR, et al. Principles and applications of diffusion-weighted imaging in cancer detection, staging, and treatment follow-up. Radiographics 2011;31(6):1773–91.

[4] Liu J-H, Tian S-F, Ju Y, Li Y, Chen A-L, Chen L-H, et al. Apparent diffusion coefficient measurement by diffusion weighted magnetic resonance imaging is a useful tool in differentiating renal tumors. BMC Cancer 2015;15(1):292.

[5] Rosenkrantz AB, Niver BE, Fitzgerald EF, Babb JS, Chandarana H, Melamed J. Utility of the apparent diffusion coefficient for distinguishing clear cell renal cell carcinoma of low and high nuclear grade. Am J Roentgenol 2010;195(5):W344–51.

[6] Cornelis F, Tricaud E, Lasserre A, Petitpierre F, Bernhard J, Le Bras Y, et al. Multiparametric magnetic resonance imaging for the differentiation of low and high grade clear cell renal carcinoma. Eur Radiol 2015;25(1):24–31.

[7] Tanaka H, Yoshida S, Fujii Y, Ishii C, Tanaka H, Koga F, et al. Diffusion-weighted magnetic resonance imaging in the differentiation of angiomyolipoma with minimal fat from clear cell renal cell carcinoma. Int J Urol 2011;18(10):727–30.

[8] Doğanay S, Kocakoc E, Cicekci M, Ağlamiş S, Akpolat N, Orhan I. Ability and utility of diffusion-weighted MRI with different b values in the evaluation of benign and malignant renal lesions. Clin Radiol 2011;66(5):420–5.

[9] Yoshikawa T, Kawamitsu H, Mitchell DG, Ohno Y, Ku Y, Seo Y, et al. ADC measurement of abdominal organs and lesions using parallel imaging technique. Am J Roentgenol 2006;187(6):1521–30.

[10] Ichikawa T, Haradome H, Hachiya J, Nitatori T, Araki T. Diffusion-weighted MR imaging with single-shot echo-planar imaging in the upper abdomen: preliminary clinical experience in 61 patients. Abdom Imaging 1999;24(5):456–61.

[11] Wu GY, Lu Q, Wu LM, WenKong, Chen XX, Xu JR. Imaging of upper urinary tract cancer: using conventional MRI and diffusion-weighted MRI with different b values. Acta Radiol 2014;55(7):882–9. http://dx.doi.org/10.1177/0284185113506576.

[12] Bozkurt M, Doganay S, Kantarci M, Yalcin A, Eren S, Atamanalp SS, et al. Comparison of peritoneal tumor imaging using conventional MR imaging and diffusion-weighted MR imaging with different b values. Eur J Radiol 2011;80(2):224–8.

[13] Göya C, Hamidi C, Bozkurt Y, Yavuz A, Kuday S, Gümüş H, et al. The role of apparent diffusion coefficient quantification in differentiating benign and malignant renal masses by 3 T magnetic resonance imaging. Balkan Med J 2015;32(3):273.

[14] Zhang J, Mazaheri Tehrani Y, Wang L, Ishill NM, Schwartz LH, Hricak H. Renal masses: characterization with diffusion-weighted MR imaging—a preliminary experience 1. Radiology 2008;247(2):458–64.

[15] Inci E, Hocaoglu E, Aydin S, Cimilli T. Diffusion-weighted magnetic resonance imaging in evaluation of primary solid and cystic renal masses using the Bosniak classification. Eur J Radiol 2012;81(5):815–20.

[16] Sevcenco S, Heinz-Peer G, Ponhold L, Javor D, Kuehhas F, Klingler H, et al. Utility and limitations of 3-Tesla diffusion-weighted magnetic resonance imaging for differentiation of renal tumors. Eur J Radiol 2014;83(6):909–13.

[17] Yu X, Lin M, Ouyang H, Zhou C, Zhang H. Application of ADC measurement in characterization of renal cell carcinomas with different pathological types and grades by 3.0 T diffusion-weighted MRI. Eur J Radiol 2012;81(11):3061–6.

[18] Wang H, Cheng L, Zhang X, Wang D, Guo A, Gao Y, et al. Renal cell carcinoma: Diffusion-weighted MR imaging for subtype differentiation at 3.0 T 1. Radiology 2010;257(1):135–43.

[19] Paudyal B, Paudyal P, Tsushima Y, Oriuchi N, Amanuma M, Miyazaki M, et al. The role of the ADC value in the characterisation of renal carcinoma by diffusion-weighted MRI. Br J Radiol 2014. Jan 28.